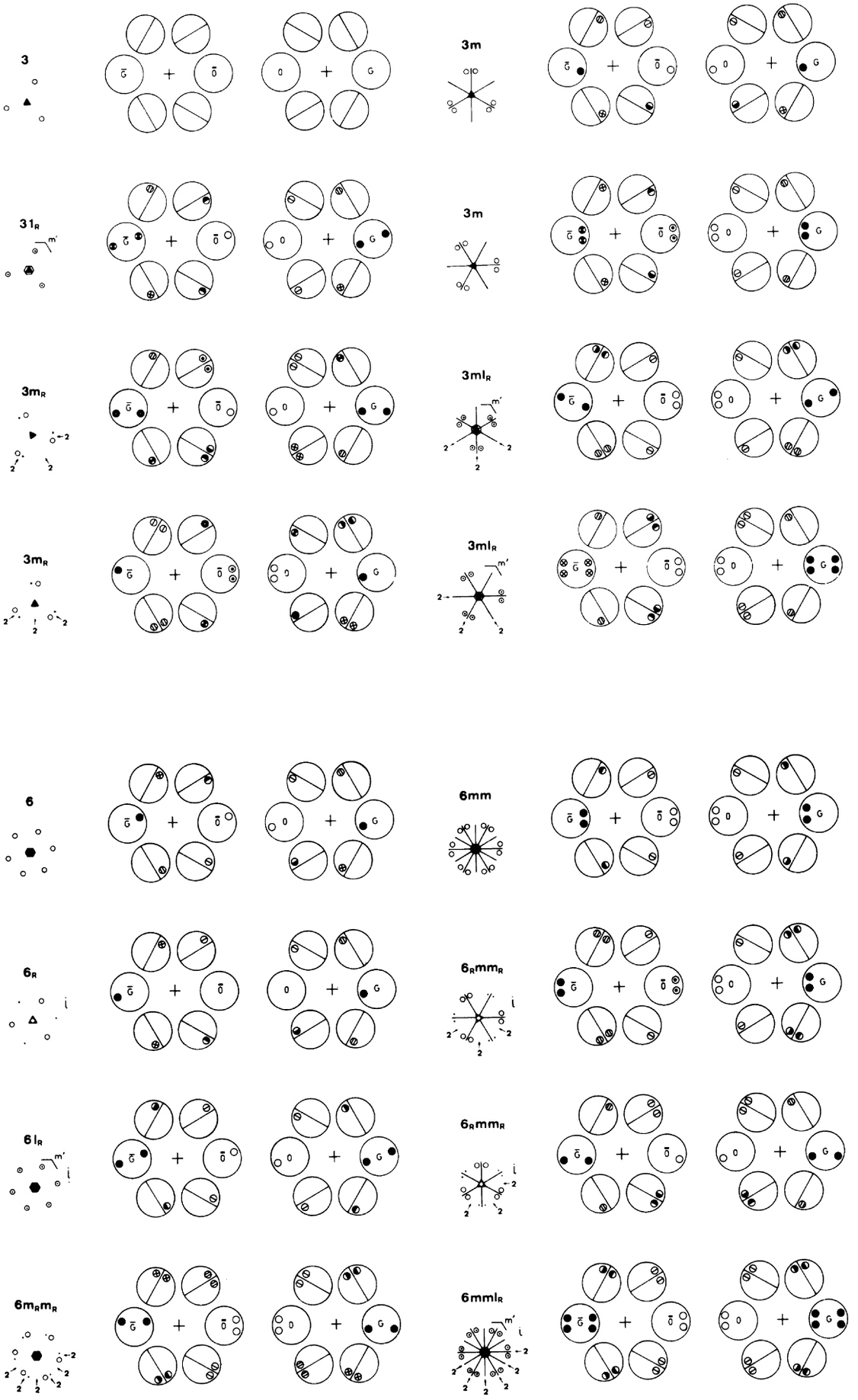


Fig. 2.5.3.7. Illustration of symmetries appearing in hexagonal six-beam, square four-beam and rectangular four-beam dark-field patterns expected for all the diffraction groups except for 1, $1_R$, 2, $2_R$ and $21_R$.

 

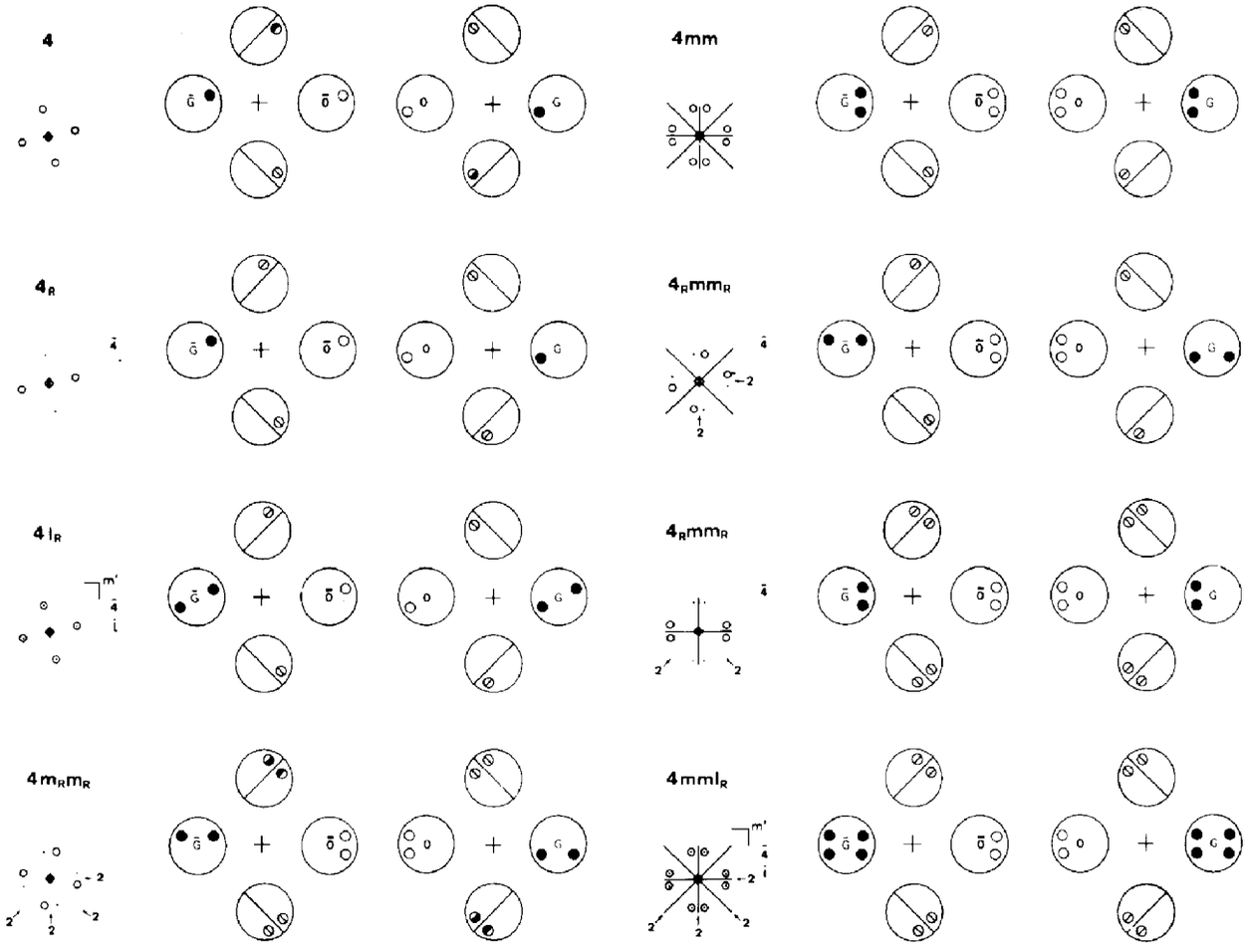


Fig. 2.5.3.7 (*cont.*).

Tables 2.5.3.5, 2.5.3.6 and 2.5.3.7 express the symmetries illustrated in Fig. 2.5.3.7 with the symmetry symbols for the hexagonal six-beam case, square four-beam case and rectangular four-beam case, respectively. In the fourth rows of the tables the symmetries of zone-axis patterns (BP and WP) are listed because combined use of the zone-axis pattern and the SMB pattern is efficient for symmetry determination. In the fifth row, the symmetries of the SMB pattern are listed. In the following rows, the symmetries appearing between the two SMB patterns are listed because the SMB symmetries appear not only in an SMB pattern but also in the pairs of SMB patterns. That is, for each diffraction group, all the possible SMB symmetries appearing in a pair of symmetric six-beam patterns, two pairs $AB$ and $AC$ of the square four-beam patterns and three pairs $AB$, $AC$ and $AD$ of the rectangular four-beam patterns are listed, though such pairs are not always needed for the determination of the diffraction groups. It is noted that the symmetries in parentheses are the symmetries which add no new symmetries, even if they are present. In the last row, the point groups which cause the diffraction groups listed in the first row are given.

By referring to Tables 2.5.3.5, 2.5.3.6 and 2.5.3.7, the characteristic features of the SMB method are seen to be as follows. CBED symmetry $m_2$ due to a horizontal twofold rotation axis can appear in every disc of an SMB pattern. Symmetry $1_R$ due to a horizontal mirror plane, however, appears only in disc $G$ or $H$ of an SMB pattern. In the hexagonal six-beam case, an inversion centre $i$ produces CBED symmetry $6_R$ between discs $S$ and $S'$ due to the combination of an inversion centre and a vertical threefold rotation axis (and/or of a horizontal mirror plane and a vertical sixfold rotation axis). This indicates that one hexagonal six-beam pattern can reveal whether a specimen has an inversion centre or not, while the method of Buxton *et al.* (1976) requires two photographs for the inversion test. All the diffraction groups in Table 2.5.3.5 can be identified from one six-beam pattern except groups 3 and 6. Diffraction groups 3 and 6 cannot be distinguished from the hexagonal six-beam pattern because it is insensitive to the vertical axis. In the square four-beam case, fourfold rotary inversion $\bar{4}$ produces CBED symmetry $4_R$ between discs $F$ and $F'$ in one SMB pattern, while Buxton *et al.*'s method requires four photographs to identify fourfold rotary inversion. Although an inversion centre itself does not exhibit any symmetry in the square four-beam pattern, it causes symmetry $1_R$ due to the horizontal mirror plane produced by the combination of an inversion centre and the twofold rotation axis. Thus, symmetry $1_R$ is an indication of the existence of an inversion centre in the square four-beam case. All of the seven diffraction groups in Table 2.5.3.6 can be identified from one square four-beam pattern. One rectangular four-beam pattern can distinguish all the diffraction groups in Table 2.5.3.7 except the groups $m$ and $2mm$. It is emphasized again that the inversion test can be carried out using one six-beam pattern or one square four-beam pattern.

Fig. 2.5.3.8 shows CBED patterns taken from a [111] pyrite ($FeS_2$) plate with an accelerating voltage of 100 kV. The space group of $FeS_2$ is $P2_1/a\bar{3}$. The diffraction group of the plate is $6_R$ due to a threefold rotation axis and an inversion centre. The zone-axis pattern of Fig. 2.5.3.8($a$) shows threefold rotation symmetry in the BP and WP. The hexagonal six-beam pattern of Fig. 2.5.3.8($b$) shows no symmetry higher than 1 in discs $O$, $G$, $F$ and $S$ but shows symmetry $6_R$ between discs $S$ and $S'$, which

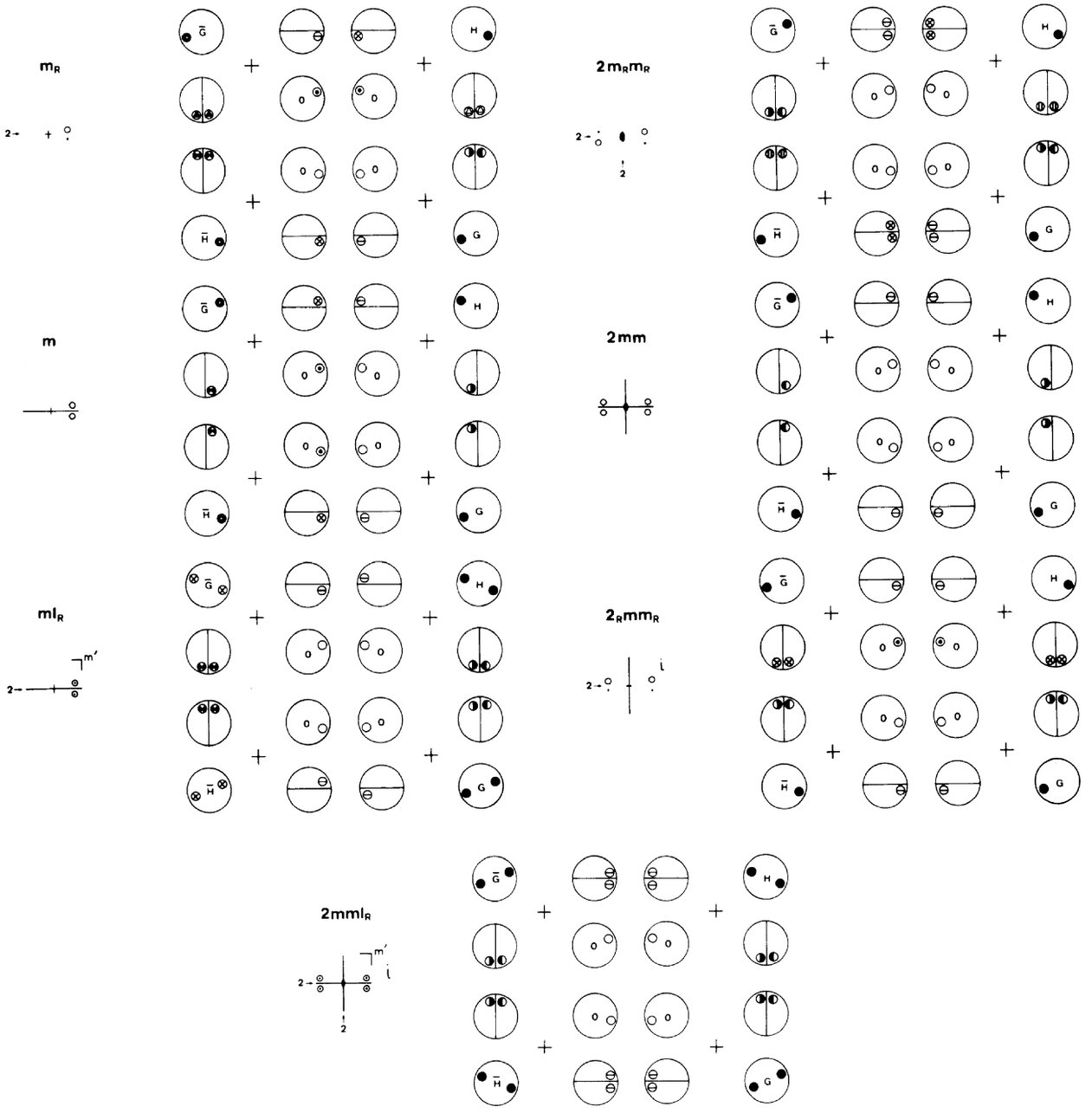


Fig. 2.5.3.7 (*cont.*).

proves the existence of a threefold rotation axis and an inversion centre. The same symmetries are also seen in Fig. 2.5.3.8(*c*), where reflections $\bar{O}$, $\bar{G}$, $\bar{F}$, $\bar{S}$, $\bar{F}'$ and $\bar{S}'$ are excited. Table 2.5.3.5 indicates that diffraction group $6_R$ can be identified from only one hexagonal six-beam pattern, because no other diffraction groups give rise to the same symmetries in the six discs. When Buxton *et al.*'s method is used, three photographs or four patterns are necessary to identify diffraction group $6_R$ (see Table 2.5.3.3). In addition, if the symmetries between Figs. 2.5.3.8(*b*) and (*c*) are examined, symmetry $2_R$ between discs $G$ and $\bar{G}$ and symmetry $6_R$ between discs $F$ and $\bar{F}$ are found. All the experimental results agree exactly with the theoretical results given in Fig. 2.5.3.7 and Table 2.5.3.5.

Fig. 2.5.3.9 shows CBED patterns taken from a [110] $V_3Si$ plate with an accelerating voltage of 80 kV. The space group of $V_3Si$ is $Pm3n$. The diffraction group of the plate is $2mm1_R$ due to two vertical mirror planes and a horizontal mirror plane, a twofold rotation axis being produced at the intersection line of two perpendicular mirror planes. The zone-axis pattern of Fig. 2.5.3.9(*a*) shows symmetry $2mm$ in the BP and WP. The rectangular four-beam pattern of Fig. 2.5.3.9(*b*) shows symmetry $1_R$ in disc $H$ due to the horizontal mirror plane and symmetry $m_2$ in both discs $\bar{S}$ and $F'$ due to the twofold rotation axes in the [001] and [110] directions, respectively. The same symmetries are also seen in Fig. 2.5.3.9(*c*), where reflections $\bar{H}$, $S'$ and $\bar{F}$ are excited. Table 2.5.3.7 implies that the diffraction group $2mm1_R$ can be identified from only one rectangular four-beam pattern, because no other diffraction groups give rise to the same symmetries in the four discs. When Buxton *et al.*'s method is used, two photographs or three patterns are necessary to identify diffraction group $2mm1_R$ (see Table 2.5.3.3). One can confirm the theoretically predicted symmetries between Fig. 2.5.3.9(*b*) and Fig. 2.5.3.9(*c*). All the experimental results agree exactly with the theoretical results given in Fig. 2.5.3.7 and Table 2.5.3.7.

These experiments show that the SMB method is quite effective for determining the diffraction group of slabs. Buxton *et al.*'s method identifies two-dimensional symmetry elements in the first place using a zone-axis pattern, and three-dimensional symmetry elements using DPs. On the other hand, the SMB method primarily finds many three-dimensional symmetry elements in an